

Solution to the slope-height ambiguity problem in phase measuring deflectometry based on a co-axial telecentric optical path

Hui-Min Yue¹, Yu-Xiang Wu², Yi-Ping Song¹ and Yong Liu¹

¹ School of Optoelectronic Information, State Key Laboratory of Electronic Thin Films and Integrated Devices, University of Electronic Science and Technology of China, Chengdu 610054, People's Republic of China

² School of Physics and Optoelectronic Engineering, Xidian University, Xi'an 710071, People's Republic of China

E-mail: yxwu@xidian.edu.cn

Received 25 July 2019, revised 16 September 2019

Accepted for publication 24 September 2019

Published 9 January 2020



CrossMark

Abstract

In recent years, phase measuring deflectometry (PMD) has become a popular method to measure the shapes of specular surfaces. However, the inherent slope-height ambiguity problem, which indicates the phase of the recorded fringe pattern is determined by both the height and slope of the test surface, causes considerable ambiguity errors in the measurement results. Existing error reduction methods usually require the initial shape information of the test surface or additional equipment to assist the measurement. These requirements make measurement inflexible in some situations. In this paper, the slope-height ambiguity problem in PMD is modelled and analyzed analytically for the first time, and the system geometry requirements of minimizing the ambiguity error are carried out accordingly. To meet these requirements, a co-axis optical path setup with a telecentric imaging system is proposed. In our simulation and experiment, this system reduces the phase and height errors by up to two orders of magnitude, compared to those from the normally employed system geometry setup.

Keywords: optical 3D imaging, optical metrology, fringe reflection technique, phase measuring deflectometry

(Some figures may appear in colour only in the online journal)

1. Introduction

With the accelerating development of science and technology, the requirement of measuring free-form specular surfaces has increased rapidly in fields ranging from optical mirror fabrication to semiconductors, mold manufacturing, and the cell phone industry [1–5]. Among all the optical three-dimensional (3D) surface metrologies, phase measuring deflectometry (PMD), which is based on structured illumination, has received much attention from researchers as it has the advantages of full-field measurement, incoherence, high sensitivity, stability and high cost performance. Its system is simply composed by a camera and a liquid crystal display (LCD) screen, while millions of points can

be measured in a single measurement with the lateral and height resolution at the micro- and nano-meter level, respectively [6–11].

However, the slope-height ambiguity problem in PMD, which indicates the extracted phase is related to both the height and the slope of the test surface, restricts the measurement accuracy of PMD. As shown in figure 1, there are an infinite combination of heights ($h_i, i = 1, 2, \dots$) and slopes (or surface normal $n_i, i = 1, 2, \dots$) of the test surface that could make the camera pixel A record the light omitted from the screen pixel B . So, because of this ambiguity problem in PMD, it is difficult to calculate the correct surface normal n_i of the tested shape if without prior knowledge of the tested shape to restrict the calculation.

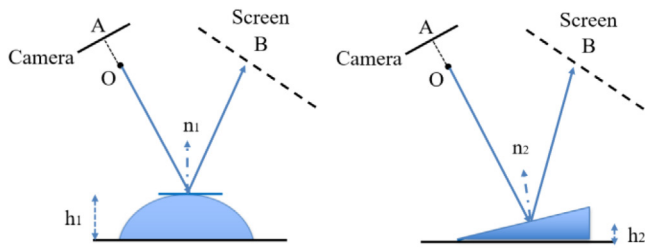


Figure 1. A schematic figure showing the slope-height ambiguity problem in PMD: two different combinations of the height and slope of a test surface may both make the camera pixel A record the light omitted from the screen pixel B.

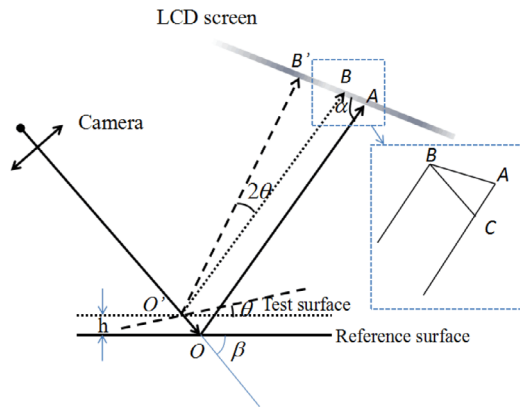


Figure 2. Schematic of the PMD system.

Existing strategies [9,12–17] for solving the slope-height ambiguity problem can be divided into two classes, which are as follows.

1. Methods with the assistance of additional equipment. In 2004, Knauer *et al* [9] solved the ambiguity problem by using an additional camera. Graves *et al* [12, 13] and Li *et al* [14] employed a laser tracking machine and point source microscope to acquire the geometry of one point on the test surface as prior knowledge. Other potential ways include using mechanical shifting stages to control the camera and LCD screen to move perpendicular to the tested mirror’s optical axis [15]. Introducing an additional component increases the uncertainty and inflexibility of the calibration of the system.
2. Methods which request prior knowledge of the test surface shape [16,17]. Sometimes it will be hard to know the shape of the test surface before testing, especially when a free-form surface is measured.

In order to suppress the measurement error caused by slope-height ambiguity, this paper firstly deduces the analytical expression of the ambiguity error caused by the slope-height ambiguity. Based on this expression, the relations between the ambiguity error and the system geometry parameters are analyzed for the first time. In this way, conditions are sought to minimize the ambiguity error. Further, a system setup based on the co-axis optical path is proposed to meet these conditions, and this system setup is proved to be feasible for suppressing error caused by the slope-height ambiguity.

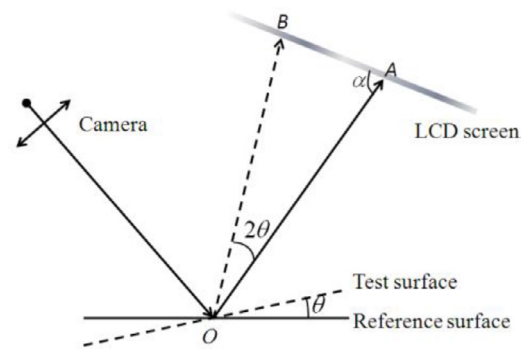


Figure 3. Schematic of the PMD system when there is only an angle difference between the test surface and reference surface.

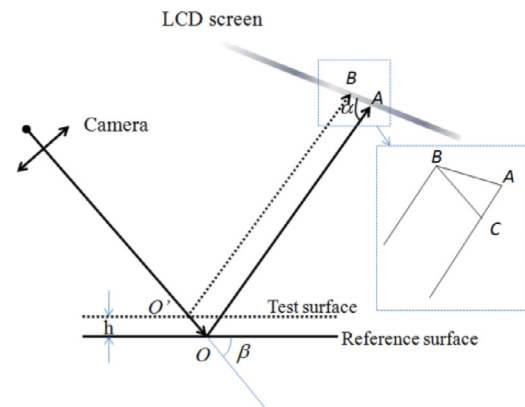


Figure 4. Schematic of the PMD system when there is only a height variation between the test surface and reference surface.

2. Analytical model of slope-height ambiguity

The schematic of the PMD system and its principle of calculating the surface slope are shown in figure 2. The camera records the fringe pattern on the LCD screen through the test specular surface. The captured fringe pattern will distort according to the height slope of the test surface. The surface slope can be calculated by establishing the relation between the phase of the distorted fringe pattern and surface slope. In figure 2, in general there is an angle difference θ between the test surface and reference surface at position O' , and there is a height difference h between them. Due to the reversibility of the optical path, the light that emits from the camera pixel is reflected by the test surface at point O' , and reaches the LCD screen at position B' . For the convenience of our analytical model’s deduction of the ambiguity error, two steps are carried out.

- a. Assume that there is an angle difference θ between the test surface and reference surface at position O , and there is no height difference between them.

Due to the reversibility of the optical path, the light that emits from the camera pixel is reflected by the reference surface at point O , and reaches the LCD screen at position A , as shown in figure 3. In $\triangle OAB$, there is

$$|AB| = \sin 2\theta \frac{|OA|}{\sin(\pi - \alpha - 2\theta)}. \quad (1)$$

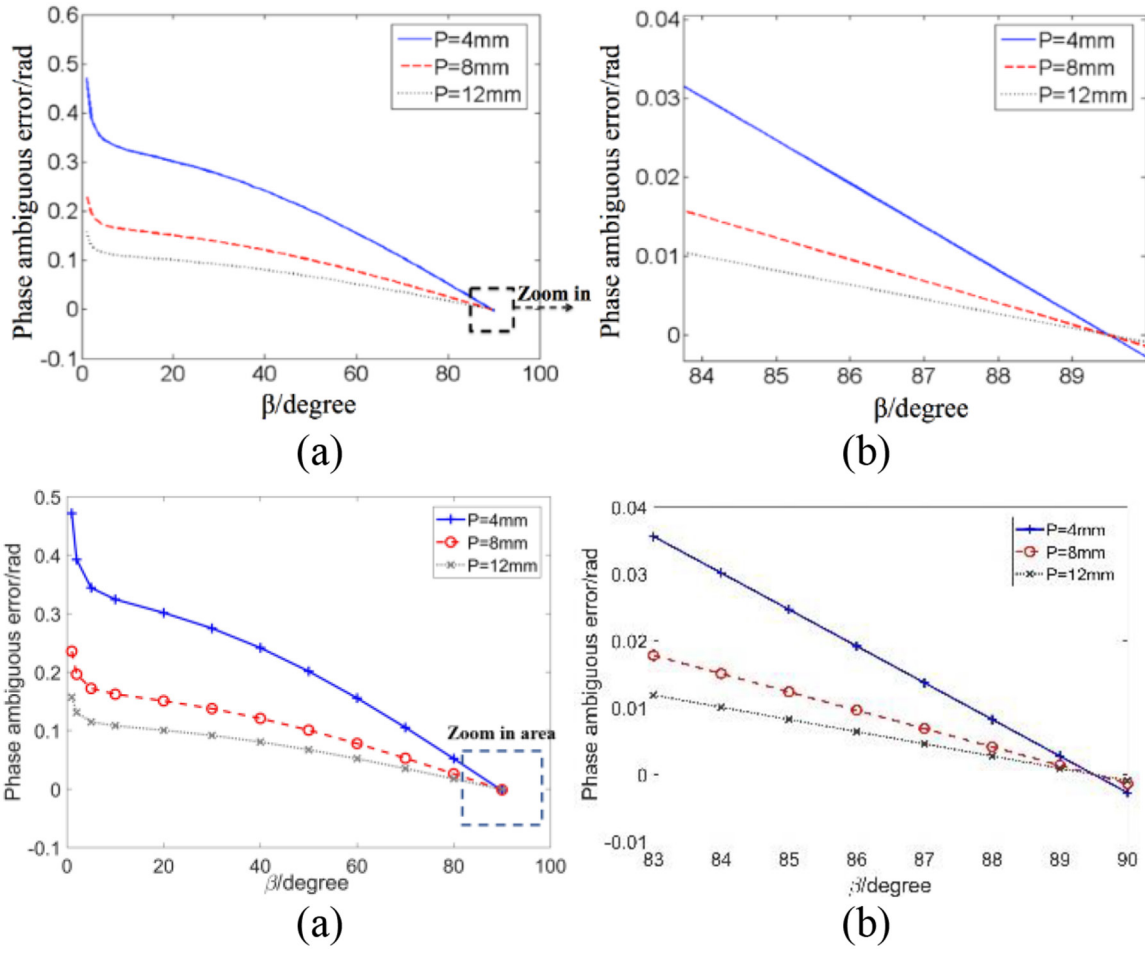


Figure 5. The influence of β on the slope-height ambiguity. (a) The relation between the phase variation caused by the slope-height ambiguity and the angle β . (b) Zoom in of the black box region in (a).

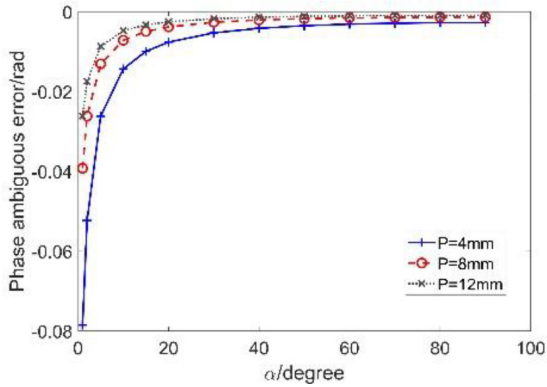


Figure 6. The relation between phase variation caused by the slope-height ambiguity and the angle α .

The phase difference between A and B is

$$\Delta\varphi = |AB| \frac{2\pi}{P}, \quad (2)$$

where P donates the period of the fringe pattern on the LCD screen. With equations (1) and (2), we have

$$\Delta\varphi = \frac{2\pi |OA| \sin 2\theta}{P \sin(\pi - \alpha - 2\theta)} = \frac{2\pi |OA| \tan 2\theta}{P(\sin \alpha + \tan 2\theta \cos \alpha)}. \quad (3)$$

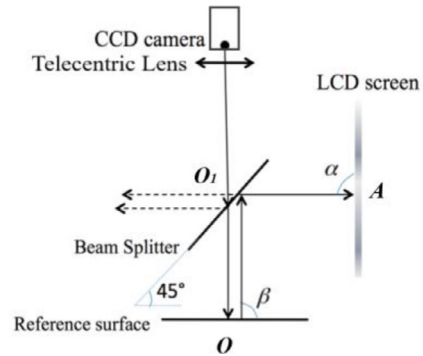


Figure 7. The setup of the proposed low slope-height ambiguity system.

b. Now suppose the test surface only has a height difference h against the reference surface, and there is no slope difference between them.

When measuring the test surface, the light will be reflected at point O' , and reach the LCD screen at position B, which is shown in figure 4. In $\triangle ABC$, the point C is chosen to satisfy $BC \parallel OO'$, and $\angle BCA = \pi - 2\beta$. So,

$$|AB| = \sin \angle BCA \frac{|BC|}{\sin \alpha} = \frac{2h \cos \beta}{\sin \alpha}. \quad (4)$$

The phase difference between A and B is

$$\Delta\varphi = \frac{4\pi h \cos \beta}{P \sin \alpha}. \quad (5)$$

As a matter of fact, the test surface has an angle difference θ against the reference surface at point O' in figure 4. However, the phase difference cannot simply be represented by equation (3) plus (5), because the $|OA|$ in equation (3) has changed to $|O'B|$ (in figure 3). $|OA|$ and $|O'B|$ have the relation of equation (6):

$$|O'B| = |OA| - |AC| = |OA| - \frac{h \sin(2\beta - \alpha)}{\sin \alpha \sin \beta}. \quad (6)$$

Therefore, the total phase variation is

$$\begin{aligned} \Delta\varphi &= \frac{4\pi h \cos \beta}{P \sin \alpha} + \frac{2\pi |O'B| \tan 2\theta}{P(\sin \alpha + \tan 2\theta \cos \alpha)} \\ &= \frac{2\pi}{P} \left\{ \frac{2h \cos \beta}{\sin \alpha} + \frac{[|OA| - \frac{h \sin(2\beta - \alpha)}{\sin \alpha \sin \beta}] \tan 2\theta}{(\sin \alpha + \tan 2\theta \cos \alpha)} \right\}. \end{aligned} \quad (7)$$

Equation (7) shows that both slope and height will affect the phase difference. We can analyze how surface height variation h affects the phase difference with equation (7).

As a slope measurement method, the phase variation in PMD is supposed to be only decided by the slope of the test surface. However, according to equation (7), the phase is also related to the height of test surface h . Without additional assumptions or restrictions to the test surface or system, it is almost impossible to distinguish the phase varied by slope and height. This is the aforementioned slope-height ambiguity problem in PMDs.

Errors will occur if we cannot eliminate the height-induced phase variation completely from the whole phase variation. It can be seen from equation (7) that the ambiguity error comes from the items containing the variable h in the right side of the equation. According to equation (7), the ambiguity error is related to the following three system parameters:

- P : the period of the fringe pattern;
- α : the angle between OA and LCD screen;
- β : the angle between the light emitted from the camera pixel and reference surface.

The relationship between the ambiguity error contained in the phase and the three system parameters will be analyzed in section 3, and an attempt is made to find the condition for minimizing the error.

3. Simulation and proposal of a low slope-height ambiguity system

The parameters in the simulation are chosen as $\alpha = 90^\circ$, $\beta = 90^\circ$, $P = 12$ mm, $h = 0.1$ mm, $\theta = 0.5^\circ$, and $|OA| = 190$ mm. Then α and β are changed gradually to see the variation of the phase caused by the slope-height ambiguity.

a. The influence of β on the slope-height ambiguity.

Figure 5(a) shows the variation trend of phase ambiguity error when the angle β changes from 1° to 90° . Figure 5(b) shows a zoom of the black box area of figure 5(a). The phase

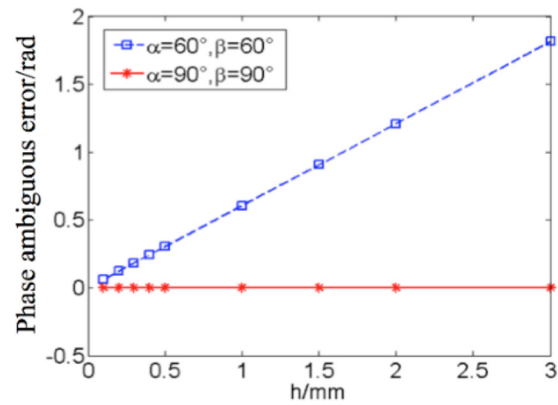


Figure 8. Simulation results of the ambiguity error in the phase in two systems (red dots are the low slope-height ambiguity system; blue dots are the typically used system).

error drops significantly with increases of the angle β . When β is increased up to 90° , the phase error is almost zero.

On the other hand, the phase ambiguity error also decreases with increases of the fringe period P , which can be deduced easily by equation (7).

b. The influence of α on the slope-height ambiguity.

Figure 6 shows the relation between phase ambiguity error and the angle α . The phase error increases rapidly when α is less than 20° , and decreases slowly when α exceeds 20° .

From the above simulation results, to minimize the phase variation caused by the slope-height ambiguity, the PMD system should satisfy the following conditions:

- (i) α and β are as close as possible to 90° ;
- (ii) the fringe period P should be increased if possible;
- (iii) a telecentric light path should be used in the imaging system, so the angle β is the same for all the rays of light.

However, with traditional optical configurations, the angle β is almost never able to attain 90° , since the camera will capture the image of the camera itself rather than the fringe pattern on the LCD screen.

In order to realize α and β values being 90° , a telecentric co-axis system is designed with the assistance of a beam splitter and a telecentric lens. The light path of this telecentric co-axis system is shown in figure 7. The angle between the beam splitter and the reference plane is 45° . The beam-splitter-based co-axis light path ensures α and β are 90° , and the purpose of the telecentric lens is to make sure each ray of light shares the same α and β values. Based on the simulation results of figures 5 and 6, compared with traditional PMD systems (when α and β are 60° as a typical value), the telecentric co-axis system in figure 7 (when α and β are 90°) will be affected less by the ambiguity problem. Further, this low-ambiguity system will be more compact in its light path because of the existence of the beam splitter.

The beam splitter should be 45° to the reference surface, and LCD screen is 90° to the reference surface. So, the angles α and β are precisely 90° . However, it can be seen from figures 5(b) and 6 that the phase variation caused by the slope-height ambiguity is still very small when there is a

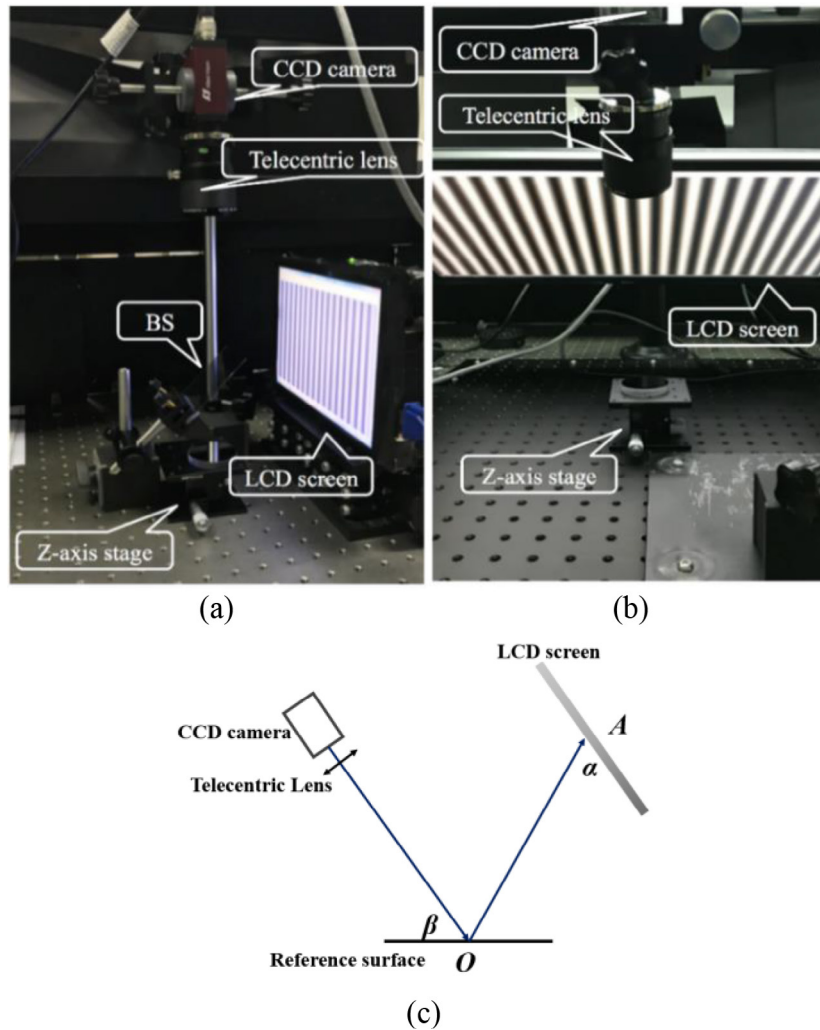


Figure 9. Experimental systems. (a) Low slope-height ambiguity system. (b) A commonly used system setup. (c) The optical configuration of the commonly employed system.

1° or 2° angle difference. In our experiment, the angles in the system are measured by a gyroscope. With the light path in figure 7, the angles α and β are close to 90° .

Simulations are undertaken to see the performance of the low slope-height ambiguity system in suppressing the ambiguity error. In this simulation, the height of the test surface is increased gradually from 0 to 3.00 mm. Then, the phase variations caused by the slope-height ambiguity in the two systems are compared, one of which is the system in figure 7, and the other the example of a commonly used system where α and β are 60° . The simulation results are shown in figure 8. The ambiguity error is consistently near 0 in the co-axis system when the surface height increases from 0 to 3.00 mm, which means the phase is barely influenced by the surface height, while in the commonly used system where α and β are 60° , the phase error increases greatly with surface height.

4. Experimental work

Figures 9(a) and (b) show the experimental setup of the low slope-height ambiguity error system and the commonly employed system. The optical configuration of figure 9(a) can

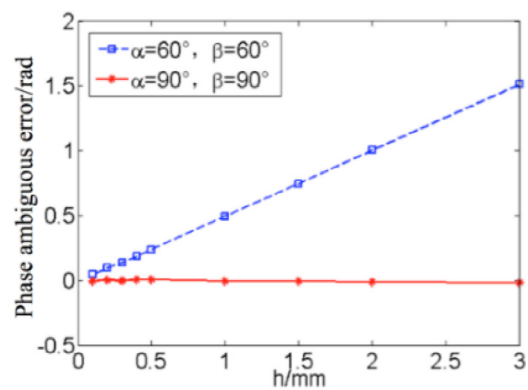


Figure 10. Experiment results of the ambiguity error in the phase in two systems. (Red dots are the slope-height ambiguity system; blue dots are the normally used system.)

be shown as figure 7. α and β are 90° . The fringe period P and the distance between reference surface and LCD screen $|OA|$ are chosen the same as their values in the simulation. It should be noted that in figure 7, $|OA| = |OO_1| + |O_1A|$. In comparison, figure 9(c) shows the optical configuration of the commonly employed system. α and β are 60° , and the P as

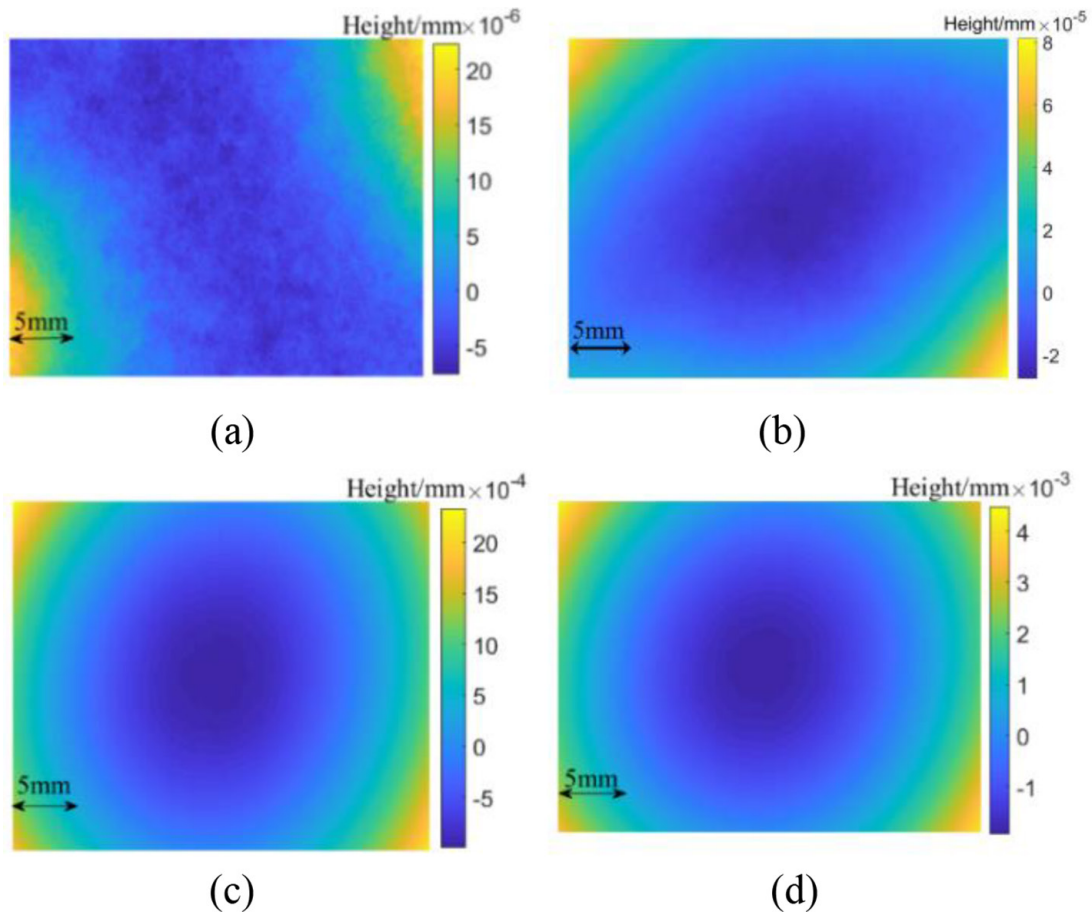


Figure 11. Experiment results of the shape error distribution when measuring a plane mirror in the proposed low slope-height ambiguity system and the normally used system. (a) With the proposed low slope-height ambiguity system and the tested mirror with 0.5 mm height difference to the reference plane; (b) with the proposed slope-height ambiguity system and the tested mirror with 1 mm height difference to the reference plane; (c) with the normally used system and the tested mirror with 0.5 mm height difference to the reference plane; (d) with the normally used system and the tested mirror with 1 mm height difference to the reference plane.

well as $|OA|$ are also chosen in accordance with their values in the simulation. In both systems, the CCD camera (Allied Vision Technologies Prosilica GT1660, with 1600×1200 pixels) is equipped with a telecentric camera lens (Computar TEC-M55).

The test surface, a plane mirror, is placed on a Z-axis stage (with a unit length of 0.01 mm). With the movement of this stage, plane mirrors with different height values are generated. The initial state of the stage is chosen as the reference plane. The phase differences caused by the test surface height variation in two systems are shown in figure 10. Comparing figure 8 (simulation result) and figure 10 (experiment result), the phase variation caused by the slope-height ambiguity in the two systems are similar both in values and trends in simulation and experiment. The ambiguity error is maintained close to zero in the slope-height ambiguity system when the surface height (Z-axis stage) increases from 0 to 3.00 mm. In contrast, the error increases greatly with the surface height in the typically used system.

Good agreement between simulation and experiment results proves the correctness of the phase error model equation (7) and the feasibility of the error suppression system setup in some degree.

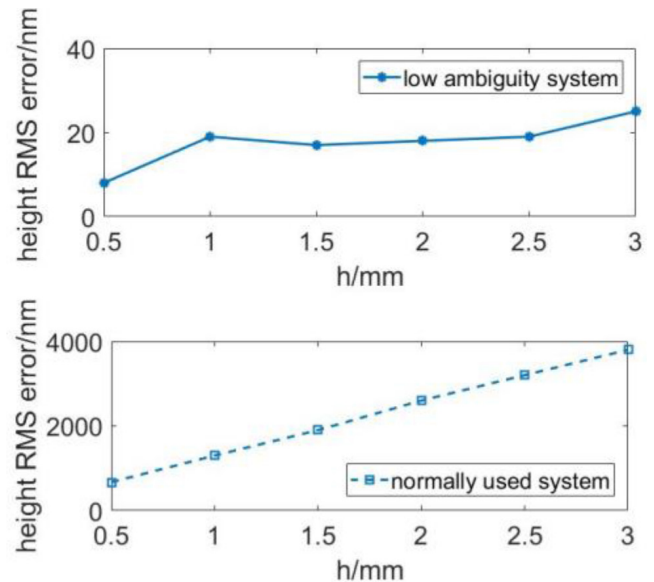


Figure 12. The measured height root mean square (RMS) error of the low slope-height ambiguity system and the normally used system when the height difference between the measured plane mirror and the reference plane increases from 0.5 mm to 3 mm.

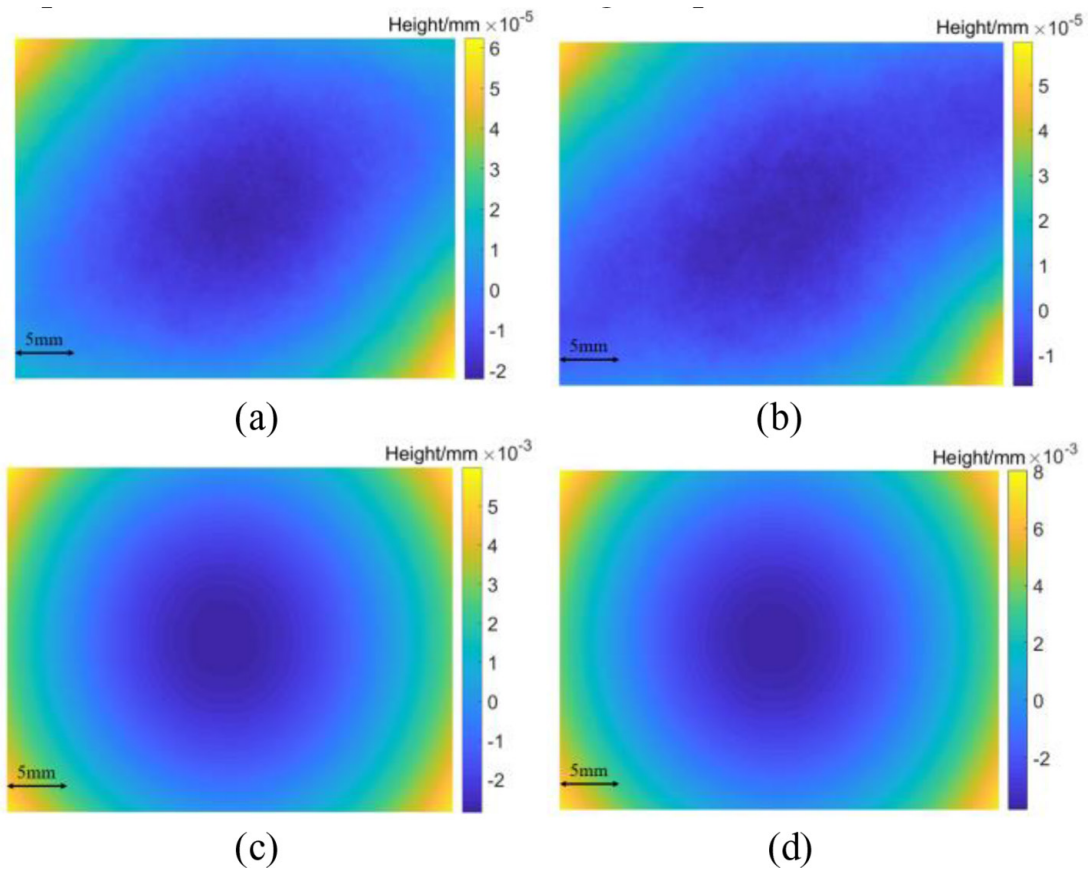


Figure 13. Experiment results of the shape error distribution when measuring a concave mirror in the proposed low slope-height ambiguity system and the normally used system. (a) With the proposed low-ambiguity system and the test mirror with 1.5 mm height difference to the reference plane; (b) with the proposed low-ambiguity system and the test mirror with 2 mm height difference to the reference plane; (c) with the normally used system and the test mirror with 1.5 mm height difference to the reference plane; (d) with the normally used system and the test mirror with 2 mm height difference to the reference plane.

Figure 11 shows the measured shape distributions of the plane mirror with 0.5 mm and 1 mm height differences to the reference plane. Figures 11(a) and (b) are the measured results of the proposed low slope-height ambiguity system, and the corresponding root mean square (RMS) values are 8.2 nm and 19 nm, respectively. Figures 11(c) and (d) are the results of the normally used system, and the corresponding RMS values are 670 nm and 1300 nm, respectively. A low slope-height ambiguity can be attained using the PMD system based on the coaxial optical path with telecentric imaging.

We further increase the height difference between the measured plane mirror and the reference plane to 1.5 mm, 2 mm, 2.5 mm, and 3 mm gradually. The height RMS error of the two systems are shown in figure 12. The proposed low ambiguity system consistently has good performance in suppressing the ambiguity error, while in the normally used system, the height RMS error increases from 670 nm to 3800 nm when the height difference between the measured plane mirror and the reference plane increases from 0.5 mm to 3 mm. The comparison of the measured shape results of the two systems are in agreement with the phase results showed in figure 10.

A concave mirror with 5000 mm radius of curvature is measured to verify the performance of the proposed method in measuring a more complex surface. The experimental procedures are in accordance with the procedures while measuring

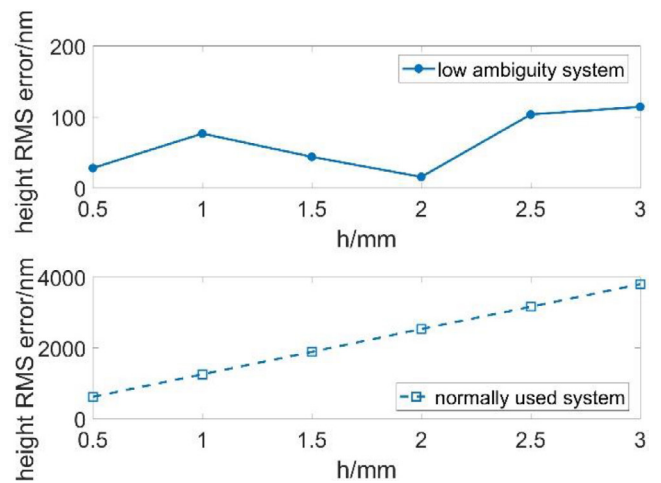


Figure 14. The measured height RMS error of the low-ambiguity system and the normally used system when the height difference between the measured concave mirror and the reference plane increases from 0.5 mm to 3 mm.

the plane mirror. Figure 13 shows the ambiguity-induced errors of the two systems when the tested mirror has 1.5 mm and 2 mm height differences to the reference plane. Figure 14 illustrates the measured height RMS error of the two systems when the height difference between the measured plane mirror

and the reference plane increases from 0.5 mm to 3 mm. For the low-ambiguity system, the ambiguity-induced errors are in the range of 17 nm to 115 nm. In contrast, the ambiguity-induced errors are in the range of 620 nm to 3780 nm for the typically employed system. These results are in accordance with the experiment results while measuring the plane mirror.

In PMDs, a reference plane mirror is often required during the system calibration or measurement procedure. With the assistance of a plane mirror, the calibration or measurement procedure can usually be simplified. However, the reference plane mirror and test mirror are required to be placed at the same spatial position, which is almost impossible in actual applications, or the ambiguity error will affect the calibration/measurement result. By using the presented low slope-height ambiguity system, the error caused by the displacement of the two surfaces will be suppressed to a very low level.

5. Conclusion

The slope-height ambiguity problem restricts the measurement accuracy of PMDs, especially in those measurement strategies with the assistance of the plane mirror. In this paper, an ambiguity error model is established. From the error's analytical expression, the relations between the ambiguity error and the system parameters are analyzed for the first time. Three conditions to minimize the ambiguity error are carried out. Moreover, a co-axis system with a telecentric light path is proposed to cope with the minimization conditions. Simulation and experiment have good agreement in showing the ability of this co-axis system in suppressing the error caused by slope-height ambiguity.

Acknowledgment

This work is funded by National Nature Science Foundation of China (Grant No. 61875035, 61805188), Sichuan Science and Technology Project (Grant No. 2018JY0579), the Fundamental Research Funds for the Central Universities (Grant No. JB180505), and the National Natural Science Foundation of Shaanxi Province (Grant No. 2019JQ-121).

ORCID iDs

Yu-Xiang Wu  <https://orcid.org/0000-0002-4490-1324>

References

- Xue S, Chen S and Tie G 2018 Near-null interferometry using an aspheric null lens generating a broad range of variable spherical aberration for flexible test of aspheres *Opt. Express* **26** 31172–89
- Zhao P, Gao N, Zhang Z, Gao F and Jiang X 2018 Performance analysis and evaluation of direct phase measuring deflectometry *Opt. Lasers Eng.* **103** 24–33
- Huang L, Xue J, Gao B, McPhersons C, Beverage J and Idir M 2017 Modal mismatch analysis and compensation for modal phase measuring deflectometry *Opt. Express* **25** 881–7
- Yan M, Huang L, Sun L and Fan J 2018 Laser thermal distortion all-time metrology system for solid-state laser based on phase measuring deflectometry *Opt. Commun.* **423** 134–9
- Huang L, Choi H, Zhao W, Graves L R and Kim D W 2016 Adaptive interferometric null testing for unknown freeform optics metrology *Opt. Lett.* **41** 5539–42
- Huang L, Idir M, Zuo C and Asundi A 2018 Review of phase measuring deflectometry *Opt. Lasers Eng.* **107** 247–57
- Niu Z et al 2018 3D shape measurement of discontinuous specular objects based on advanced PMD with bi-telecentric lens *Opt. Express* **26** 1615–32
- Xu Y, Gao F and Jiang X 2018 Performance analysis and evaluation of geometric parameters in stereo deflectometry *Engineering* **4** 806–15
- Knauer M C, Kaminski J and Häusler G 2004 Phase measuring deflectometry: a new approach to measure specular free-form surfaces *Proc. SPIE* **5457** 366–76
- Wu Y X, Yue H M, Yi J Y, Li M Y and Liu Y 2016 Dynamic specular surface measurement based on color-encoded fringe reflection technique *Opt. Eng.* **55** 0241041–7
- Zhu R G, Zhu R H, Song Q and Li J 2013 Specular surface measurement based on fringe reflection and study on 3D shape reconstruction technique *Proc. SPIE* **8769** 87692S
- Graves L R et al 2018 Model-free deflectometry for freeform optics measurement using an iterative reconstruction technique *Opt. Lett.* **43** 2110–3
- Zhao W et al 2016 Iterative surface construction for blind deflectometry *Proc. SPIE* **9684** 96843X
- Li W, Sandner M, Gesierich A and Burke J 2012 Absolute optical surface measurement with deflectometry *Proc. SPIE* **8494** 84940G
- Tang Y, Su X Y, Liu Y K and Jing H 2008 3D shape measurement of the aspheric mirror by advanced phase measuring deflectometry *Opt. Express* **16** 15090–6
- Huang L, Xue J, Gao B, McPhersons C, Beverage J and Idir M 2016 Modal phase measuring deflectometry *Opt. Express* **24** 24649–64
- Huang L, Chi S and Asundi A K 2012 Fast full-field out-of-plane deformation measurement using fringe reflectometry *Opt. Lasers Eng.* **50** 529–33